Vol. 448: 39–49, 2012
doi: 10.3354/meps09490

MARINE ECOLOGY PROGRESS SERIES
Mar Ecol Prog Ser

Published February 23

OPEN ACCESS

Effect of Typhoon Morakot on microphytoplankton population dynamics in the subtropical Northwest Pacific

Chih-Ching Chung[1,2,*], Gwo-Ching Gong[1,2], Chin-Chang Hung[1,3]

[1]Institute of Marine Environmental Chemistry and Ecology, and [2]Center of Excellence for Marine Bioenvironment and Biotechnology, National Taiwan Ocean University, 20224 Keelung, Taiwan

[3]Institute of Marine Geology and Chemistry, National Sun Yat-sen University, 80424 Kaohsiung, Taiwan

ABSTRACT: Satellite ocean color imagery indicates that typhoons enhance sea surface chlorophyll concentrations along their paths. However, the influence of typhoons on microphytoplankton community dynamics is still poorly understood because of the risk of sampling at sea under extreme weather conditions. From 22 July to 26 August, 2009, before and after the passage of the devastating Typhoon Morakot (7–9 August), 7 field cruises were conducted at a station in the southern East China Sea, northeast of Taiwan. Microphytoplankton species composition and related hydrographic and nutrient samples were analyzed. The diatom abundance increased by approximately 50 times just 10 d after the passage of Morakot, and the diatom population was dominated by chain-forming centric diatoms (*Chaetoceros* spp.) instead of the *Trichodesmium* and *Gymnodinium* spp. that prevailed before the typhoon. The strong winds and heavy rains of Morakot caused nutrient entrainment from upwelling and nutrient-enriched floodwaters with a low N:P ratio, driving the observed diatom bloom and change in species composition. The diatom bloom was terminated within 24 h. Based on the concurrent increase in copepods, we suggest that intensive grazing pressure was the main cause of the termination of the diatom bloom induced by Typhoon Morakot.

KEY WORDS: Typhoon · Microphytoplankton · Bloom dynamics · Morakot · East China Sea · Kuroshio Current

INTRODUCTION

Episodic environmental events, such as dust storms and cyclones, induce large-scale ocean–atmosphere interactions and have profound influences on phytoplankton ecology, as well as on biogeochemical cycles (Karl et al. 2001, Jickells et al. 2005, Falkowski & Oliver 2007). For example, aeolian deposition and strong water mixing accompanied by Asian dust storm events provide nutrients that stimulate picophytoplankton growth, subsequently enhancing the particulate organic carbon (POC) export flux in the subtropical Northwest Pacific Ocean (Hung et al. 2009, Chung et al. 2011). Typhoons (also known as tropical cyclones or hurricanes) are classified as severe climate events in tropical and subtropical provinces. After a typhoon has passed, increases in phytoplankton blooms and primary production in coastal regions have frequently been observed (Chang et al. 1996, Shiah et al. 2000, Paerl et al. 2006). A similar consequence in the open ocean has also been inferred from satellite ocean color imagery and modeling (Walker et al. 2005, Shi & Wang 2007, Chang et al. 2008, Zhao et al. 2008, Siswanto et al. 2009). Recent analyses of past typhoons have suggested that global warming will lead to increasing

*Email: chungcc@mail.ntou.edu.tw

intensity of the strongest typhoons and that the impacts of typhoons on oceanic biogeochemistry will also be augmented (Elsner et al. 2008, Hoegh-Guldberg & Bruno 2010).

Strong winds and heavy precipitation are the major influencing factors accompanying typhoons (Zheng & Tang 2007, Chen et al. 2009). Nutrients pumped from deep water by strong wind-induced vertical mixing, upwelling, or both clearly enhance chlorophyll *a* (chl *a*) concentrations in the open ocean (Vinayachandran & Mathew 2003, Babin et al. 2004, Walker et al. 2005, Shi & Wang 2007, Zheng & Tang 2007, Chang et al. 2008, Siswanto et al. 2009, Byju & Kumar 2011, Hung & Gong 2011). In addition to the effects of strong winds, river discharge from the areas of typhoon-induced floods also contributes a considerable amount of terrestrial organic materials to the oceans (West et al. 2011). The effects of abrupt terrestrial nutrient influx on phytoplankton growth and primary productivity are usually constrained to estuarine and coastal waters (Chang et al. 1996, Shiah et al. 2000, Paerl et al. 2006, Gong et al. 2011). Nevertheless, Chen et al. (2009) reported that the enrichment of riverine nutrients after the passage of typhoons affected phytoplankton assemblages and primary productivity in the upper Kuroshio Current. Moreover, the storm-induced eddy entrained the nutrient-rich waters from the Mississippi River discharges to the open Gulf of Mexico and subsequently led to phytoplankton blooms (Yuan et al. 2004).

On average, at least 26 typhoons occur in the northwest Pacific Ocean and South China Sea every year (Central Weather Bureau, Taiwan, www.cwb.gov.tw). Unfortunately, extreme weather conditions during the pre- and post-typhoon periods make it difficult to conduct frequent measurements at sea, especially in offshore areas (Chang et al. 1996). Although numerous studies have documented the effects of typhoons on primary productivity and phytoplankton ecology in the open ocean, most of these conclusions have been inferred from satellite remote sensing data. Chl *a* values derived from satellite color images may be misleading due to the change in phytoplankton composition or the presence of suspended particles and chromophoric dissolved organic matter (Hoge & Lyon 2002, Shang et al. 2008, Tang et al. 2008, Hung et al. 2010). Additionally, cloudy weather accompanying a typhoon event interrupts the acquisition of satellite ocean color imagery. Although Hung et al. (2010) conducted a survey in the southern East China Sea, which included satellite remote sensing, modeling, and field measurements, to examine the role of typhoons in determining ocean properties and POC flux, the authors did not report the hydrographic conditions that were present before typhoons. It is difficult to elucidate the detailed ocean biogeochemical processes affected by typhoons without frequent *in situ* field observations both pre- and post-cyclone.

From 7 to 9 August 2009, Typhoon Morakot swept over northern Taiwan and drenched southern Taiwan with record-breaking rainfall that exceeded 2000 mm in 3 d. This devastating typhoon resulted in 685 people dead and missing, as well as losses in agriculture and fisheries totaling over US$0.6 billion in southern Taiwan. Morakot was the most severe natural disaster in Taiwan in the last 50 yr (Hong et al. 2010; Central Weather Bureau, Taiwan, www.cwb.gov.tw). We took this opportunity to conduct 7 cruises during the pre- and post-cyclone periods to study the influence of typhoons on hydrographic properties and the population dynamics of microphytoplankton (cell sizes between 20 and 200 µm) in the subtropical coastal Northwest Pacific. This time series of sea-based observations will help us to gain a comprehensive understanding of the influence of typhoons on coastal oceans.

MATERIALS AND METHODS

Sampling

An observation station (25.45° N, 122.00° E), located approximately 70 km northeast of Taiwan, was established at the continental shelf break in the southern East China Sea (Fig. 1). The bottom depth at this station is 130 m. Hydrographic features in this area are greatly affected by the intrusion of the Kuroshio subsurface water and the northeastward warm Taiwan Strait outflow, called the Taiwan Current Warm Water in this study (TCWW; Fig. 1). During the periods before and after Morakot, a total of 7 cruises were conducted. Five cruises aboard RV 'Ocean Researcher II' ('ORII') were made on the following dates: 22 July, 5 August, 11–12 August, 18–19 August, and 25–26 August. The other 2 cruises were conducted on 14 and 16 August aboard the fishing boat 'Yang-Ming.' Aboard the 'ORII,' water temperature and salinity were measured with a conductivity/temperature/depth (CTD) recorder (SBE911 plus, SeaBird). Surface salinity and temperature along the ship track were continuous recorded by a surface thermosalinograph (SBE21, SeaBird). Particle transmission in different water layers was measured with a transmissometer (Wet

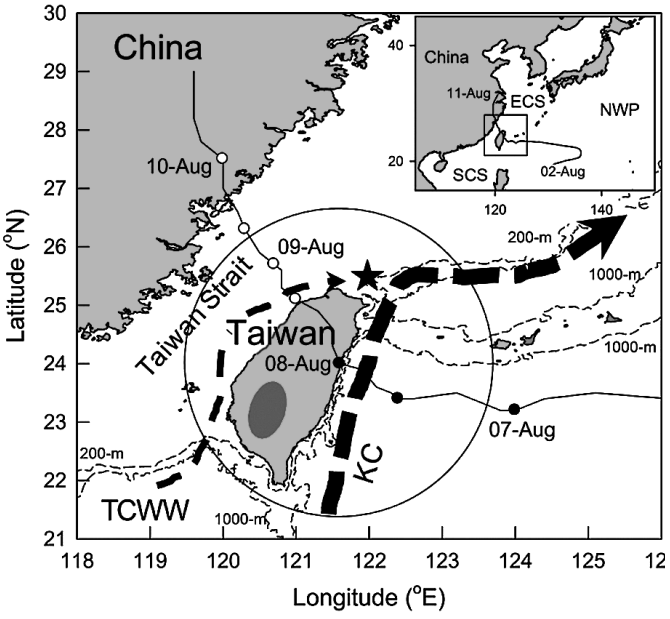

Fig. 1. Track of Typhoon Morakot and the location of the observation station in the southern East China Sea. The complete route of Morakot from 2 to 11 August is shown in the upper right panel. NWP, ECS, and SCS denote the Northwestern Pacific, the East China Sea, and the South China Sea, respectively. The small solid and open circles denote the strength of Morakot at levels of category-2 (maximum wind speed = 43 m s^{-1}) and category-1 (maximum wind speed = 33 m s^{-1}), respectively. The large circle represents the area where the wind speed was above 14 m s^{-1}. The arrows indicate the flow directions of the Kuroshio Current (KC) and the Taiwan Current Warm Water (TCWW; Gong et al. 1996, Jan et al. 2010, 2011). The location of the observation station is indicated by a star. The Morakot-induced flooding region in southern Taiwan is shaded dark gray

Labs). Underwater irradiance was recorded with a photosynthetically active radiation (PAR) scalar quantum irradiance sensor (Chelsea Technologies Group). The mean light attenuation coefficient (Kpar) was obtained from a linear regression of the logarithm-transformed profiles of underwater irradiance. The depth of the euphotic zone was determined by the depth at which the light intensity was 1% of the surface irradiance (Lorenzen 1972, Gong et al. 1999). The bottom of the mixed layer was defined as the depth at which the temperature was 0.5°C lower than that at the surface (Levitus 1982). Samples were collected using 20 l Niskin bottles mounted on the CTD rosette. Aboard the 'Yang-Ming,' water samples from specific depths in the water column were collected using a 10 l Niskin bottle connected with a nylon rope. The water samples were further processed for microplanktonic cell enumeration and determination of chl *a* and nutrient concentrations as described below.

Microphytoplankton cell enumeration

Each liter of sea water collected from the surface layer and at a depth of 50 m was immediately preserved with acidic Lugol's solution at a ratio of 1:100 (v:v). The microplankton cells in the water samples were settled by gravity in the dark for approximately 1 mo. The supernatant was carefully withdrawn by an aspirator until 50 ml remained in the bottle. Then 1 ml of the concentrated water sample was transferred into a Sedgwick-Rafter counting disk. Microphytoplanktonic cells in the counting disk were identified and counted at 200× magnification with a microscope (Axio, Zeiss) (Chang et al. 2000). Dinoflagellates and diatoms were identified to the genus level based on Tomas et al. (1996). Copepods and their fecal pellets were also enumerated. The indices of microphytoplankton diversity (H') and evenness (J') were calculated according to the following equations (Shannon 1948, Pielou 1966):

$$H' = -\sum_{i=1}^{S} P_i \ln P_i \qquad (P_i = \frac{N_i}{N}) \tag{1}$$

$$J' = \frac{H'}{\ln S} \tag{2}$$

where S = the total number of species, N = the total abundance of organisms, and N_i = the number of individuals of species i.

Determination of chl *a* and nutrient concentrations

Chl *a* samples were collected by filtering 500 ml of sea water through a 47 mm diameter GF/F filter (Whatman) and were stored at −20°C until analysis. Chl *a* that was retained on the filter was extracted with 90% acetone and then measured with a fluorometer (Model 10-AU-005, Turner Design) (Parsons et al. 1984, Gong et al. 2000).

For the nutrient analyses, water samples in 100 ml polypropylene bottles were quickly frozen in liquid nitrogen and then stored at −20°C until analysis. The methods employed for the analyses of nutrients, namely nitrate (NO_3), nitrite (NO_2), phosphate (PO_4), and silicate (SiO_4), are described in detail elsewhere (Gong et al. 2000, 2003).

RESULTS

Physical and chemical hydrographic properties

Morakot was a category-2 typhoon with a maximum sustained wind speed of 40 m s^{-1}. The ty-

Table 1. Hydrographic information before and after Typhoon Morakot. Parameters listed are temperature (T), salinity (S), depth of the euphotic zone (EZ, 1% of surface light intensity), turbidity (TM), nitrate (NO_3), nitrite (NO_2), phosphate (PO_4), silicate (SiO_4) and chlorophyll *a* (chl *a*) concentrations in the surface water. I(N+N) and I(chl *a*) are the concentrations of NO_3+NO_2 and chl *a* integrated from the surface to a depth of 50 m. na: data not available

Date	T (°C)	S (PSU)	EZ (m)	TM (%)	NO_3 (µM)	NO_2 (µM)	I(N+N) (mmol m^{-2})	PO_4 (µM)	SiO_4 (µM)	Chl *a* (mg m^{-3})	I(chl *a*) (mg m^{-2})
22 Jul	27.9	33.6	41	93.6	0.0	0.0	140.7	0.1	2.6	0.4	36
05 Aug[a]	30.3[b]	33.4[b]	na	na	0.5	0.0	na	0.0	2.1	0.3	na
After Morakot (landfall on Taiwan on 8 August)											
11 Aug	22.9	34.0	na	85.3	5.1	0.3	348.6	0.3	11.6	1.2	25
12 Aug	27.1	33.7	na	86.5	0.4	0.1	160.6	0.1	3.7	1.6	69
14 Aug[c]	26.6	33.2	na	na	0.8	0.5	121.4	0.2	6.0	1.9	103
16 Aug[c]	27.7	33.0	na	na	0.3	0.1	47.5	0.3	4.7	na	na
18 Aug	27.8	32.3	29	71.2	0.3	0.6	129.1	0.3	4.8	3.7	71
19 Aug	28.5	32.3	32	94.9	0.6	0.5	121.5	0.1	4.1	0.8	46
26 Aug	27.8	33.3	45	95.9	0.4	0.1	85.5	0.0	4.0	0.7	37

[a]Only surface water samples were obtained
[b]Values of temperature and salinity were measured by surface thermosalinograph (SBE21, SeaBird)
[c]Observations conducted onboard a fishing boat

phoon made landfall on the northeastern coast of Taiwan on 8 August 2009 and remained over the island for 12 h (Fig. 1). The disturbances (wind and precipitation) caused by Morakot occurred not only directly along its progressing path. In addition to the strong wind that swept over northern Taiwan, Morakot also carried record-breaking rainfall into southern Taiwan. Within 2 d (8 and 9 August), freshwater in excess of 1.5×10^{10} m^3 from the flooding areas was injected into the southern Taiwan Strait (Water Resource Bureau, Taiwan, www.wra.gov.tw; Fig. 1).

On 22 July, the water temperature was 27.9°C in the surface layer and 16.6°C at 100 m. The vertical variation in salinity ranged from 33.6 to 34.5 (Table 1, Fig. 2A). The surface salinity along the ship track from the Keelung Harbor to the study site also remained at higher values between 33.0 and 33.5 (Fig. 3). The concentrations of dissolved inorganic nitrogen (DIN: NO_2+NO_3), dissolved inorganic phosphate (DIP), and silicate (SiO_4) were at low or undetectable levels in the mixed layer (Table 1, Fig. 4A,B). The hydrographic features on 22 July fit within previous surveys (Gong et al. 2000, Liu et al. 2010)

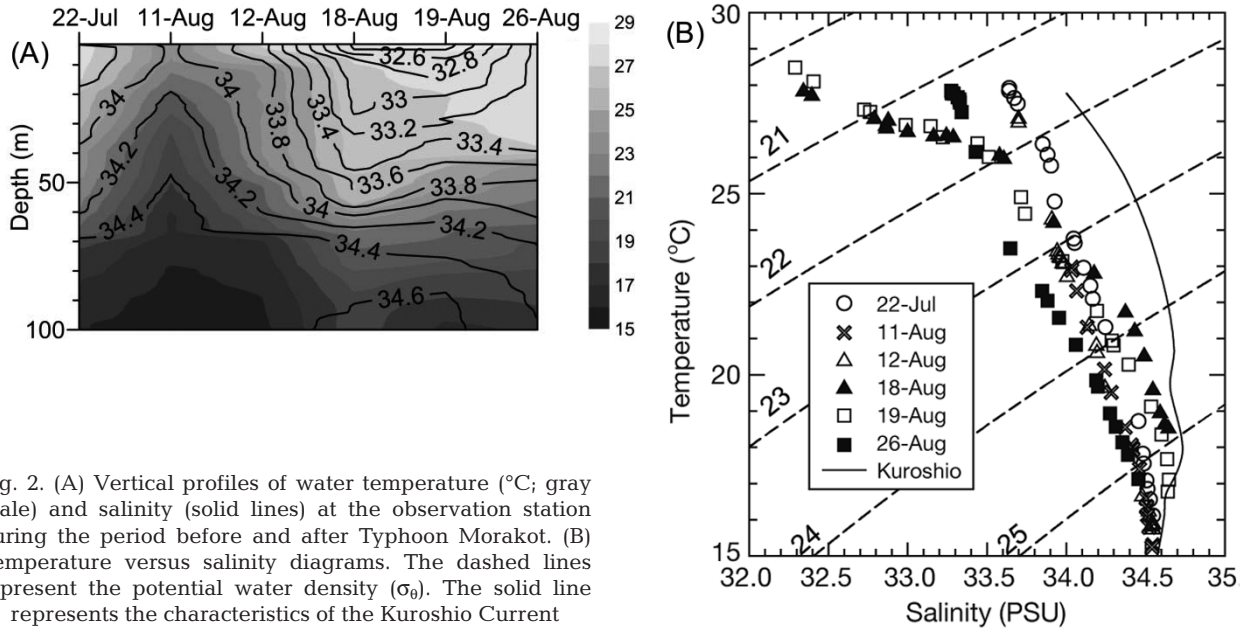

Fig. 2. (A) Vertical profiles of water temperature (°C; gray scale) and salinity (solid lines) at the observation station during the period before and after Typhoon Morakot. (B) Temperature versus salinity diagrams. The dashed lines represent the potential water density (σ_θ). The solid line represents the characteristics of the Kuroshio Current

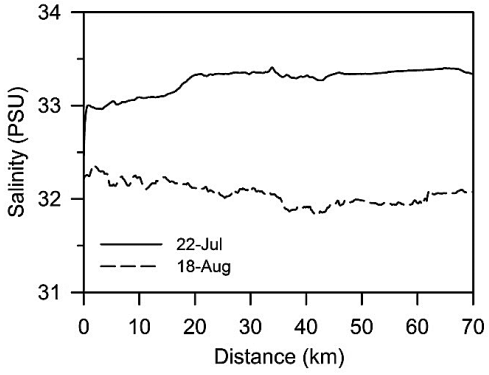

Fig. 3. Surface salinity along the ship track from the north coast of Taiwan at Keelung Harbor (25.17° N, 121.80° E) to the study site. The salinities pre- and post-Typhoon Morakot are denoted by the solid and dashed lines, respectively

and represented the typical states without episodic disturbances.

Following the passage of Morakot, the hydrographic properties changed significantly. The temperature–salinity (T–S) diagrams clearly reveal the occurrences of upwelling and the consecutive influx of lower-salinity water at the observation site (Fig. 2). On the third day after Morakot (11 August), deep nutrient-rich water was brought to the surface, derived from the Kuroshio upwelling. The surface temperature dramatically declined to 22.9°C, and the salinity in the entire water column remained high at 34 to 34.5 (Fig. 2). Moreover, the surface concentrations of DIN, DIP, and SiO_4 were at high values of 5.4, 0.3, and 11.6 µM, respectively (Table 1, Fig. 4A,B). On 12 August, the upwelling event terminated. The water column was stratified with a clear thermocline, where the temperatures decreased from 27°C at the surface to 23°C at a depth of 10 m (Fig. 2A). The DIN and DIP concentrations in the mixed layer quickly declined to undetectable levels within 24 h (Fig. 4A,B).

The water masses with lower salinity (<33) were found over the surface layer on 18 and 19 August (Fig. 2). The surface salinity along the ship track also followed a similar trend (Fig. 3). However, the vertical sections of DIN, DIP, and SiO_4 revealed that the terrestrial nutrient influx initially emerged in the surface layer on 14 August and gradually occupied the upper 50 m of the water column on 18 August (Fig. 4A,B). Great amounts of dissolved nutrients were carried with the lower-salinity water intrusion. In particular, the surface DIP concentrations remained at high levels, more than 0.2 µM, during the period between 16 and 18 August (Fig. 4B). Subsequently, this lower-salinity water mass gradually mixed with the oceanic water. The hydrographic features on 26 August had returned to the conditions present before Morakot passed except that the depth of the mixed layer increased to 32 m, and the lower surface salinity was 33.3 (Table 1, Figs. 2 & 4A,B).

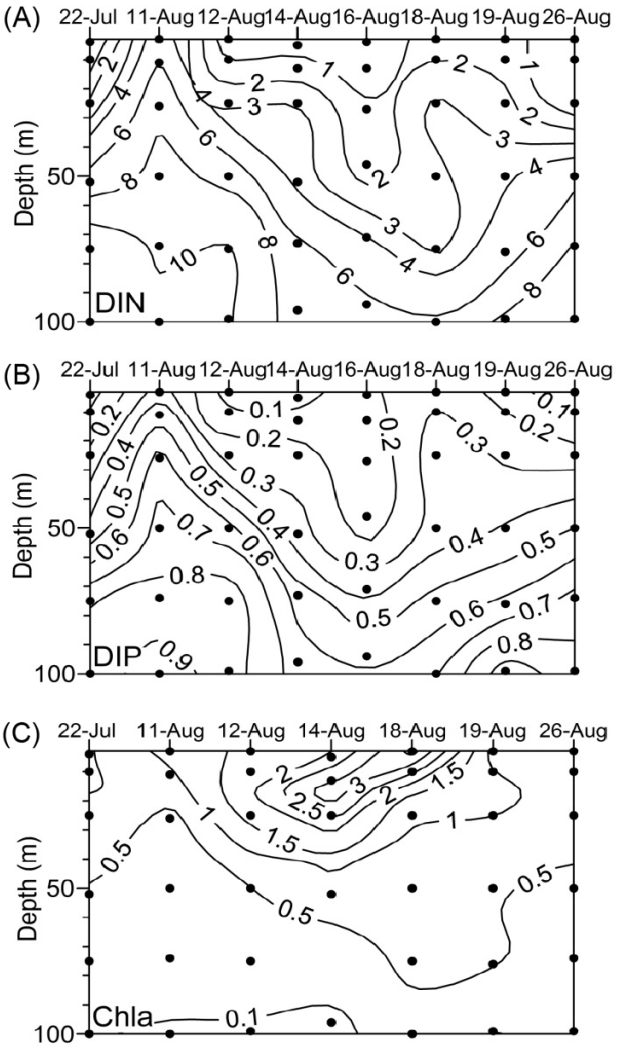

Fig. 4. Vertical profiles of the concentrations of (A) dissolved organic nitrogen (DIN, NO_3 + NO_2), (B) dissolved inorganic phosphate (DIP), and (C) chlorophyll *a* (chl *a*). No profile of chl *a* concentration was obtained on 16 August

Chl *a* concentration and microphytoplankton composition

On 22 July and 5 August, before the passage of Morakot, the surface water was clear with a particle transmission of 93.6%, and the bottom of the euphotic zone was at 41 m (Table 1). The chl *a* concentration at the surface layer was between 0.3 and 0.4 mg m^{-3} (Table 1). The chl *a* maximum was located

Table 2. Surface microphytoplankton assemblages during the periods before and after Typhoon Morakot passed. Note that the abundance of *Trichodesmium* is presented as trichomes l^{-1}

	Genus	Abundance (cells l^{-1})							
		05 Aug	11 Aug	12 Aug	14 Aug	16 Aug	18 Aug	19 Aug	26 Aug
Centric diatoms	*Bacteriastrum*	0	0	0	140	0	2950	0	0
	Chaetoceros	0	960	480	12360	47800	171750	1710	90
	Ditylum	0	10	0	40	0	0	10	0
	Eucampia	0	50	0	0	0	0	0	0
	Guinardia	0	110	30	100	100	1350	0	0
	Rhizosolenia	30	0	0	0	0	100	0	80
	Skeletonema	0	400	70	3240	1120	1400	50	0
Pennate diatoms	*Cylindrotheca*	0	240	0	0	0	0	0	0
	Navicula	0	0	0	0	0	0	0	420
	Nitzschia	0	3100	230	12740	17060	13650	750	1030
	Thalassionema	0	570	590	960	1780	2000	670	130
Dinoflagellates	*Ceratium*	50	10	10	40	0	0	0	0
	Dinophysis	30	0	10	0	0	50	0	10
	Gymnodinium	1360	140	370	400	0	0	0	0
	Protocentrum	50	40	80	3420	200	100	0	10
	Protoperidinium	20	10	40	40	7380	4700	80	260
Cyanobacterium	*Trichodesmium*	860	30	130	10	180	0	0	20

at 25 m at a concentration of 1.2 mg m^{-3} (Fig. 4C). After Morakot passed, the chl *a* maximum was elevated to the surface with the upwelling event. Subsequently, the surface chl *a* concentration increased from 1.6 to 1.9 mg m^{-3}. The integrated concentrations of chl *a* (Ichl*a*, i.e. the concentration of chl *a* integrated from the surface to a depth of 50 m) also showed a significant increase from 24.6 mg m^{-2} on 11 August to 103 mg m^{-2} on 14 August (Table 1, Fig. 4C). On 18 August, the surface chl *a* concentration reached a maximum value of 3.7 mg m^{-3} and subsequently rapidly declined to 0.8 mg m^{-3} within 24 h. The surface particle transmission rebounded from 71.2 to 94.9%, which corresponded with the change in surface chl *a* concentration (Table 1, Fig. 4C).

The assemblages of microphytoplankton differed pre- and post-typhoon. Before Morakot, the microphytoplankton in the surface water was mainly composed of small dinoflagellates, such as *Gymnodinium* spp. and the diazotrophic filamentous cyanobacteria *Trichodesmium* spp. (Table 2). After Morakot passed, diatoms gradually became the dominant microphytoplankton. On 11 August, the assemblage of microphytoplankton was composed of pennate diatoms (e.g. *Nitzschia* spp. and *Thalassionema* spp.). Subsequently, there was an increase not only in the abundance of pennate diatoms but also of large chain-forming centric diatoms, such as *Bacteriastrum* spp., *Chaetoceros* spp., and *Skeletonema* spp., which gradually thrived in the surface water. During the period between 12 and 16 August, the species compositions of microphytoplankton were more diverse (Table 2, Fig. 5). On 18 August, *Chaetoceros* spp. reached a maximum abundance of 1.7 × 10^5 cells l^{-1}. The cell numbers of pennate diatoms also remained at the highest levels, but their total abundance was 10 times lower relative to centric diatoms (Table 2). The lowest indices of diversity and evenness corresponded to the thriving of *Chaetoceros* (Fig. 5). Moreover, the greatest abundance of copepods, which was 350 ind. l^{-1}, was also ob-

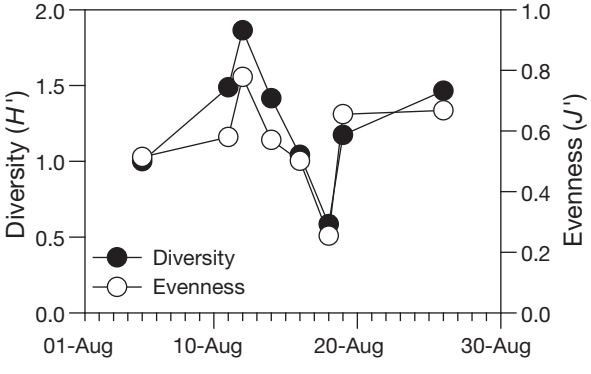

Fig. 5. Indices of biological diversity (*H'*) and evenness (*J'*) for the assemblages of microphytoplankton pre- and post-Typhoon Morakot

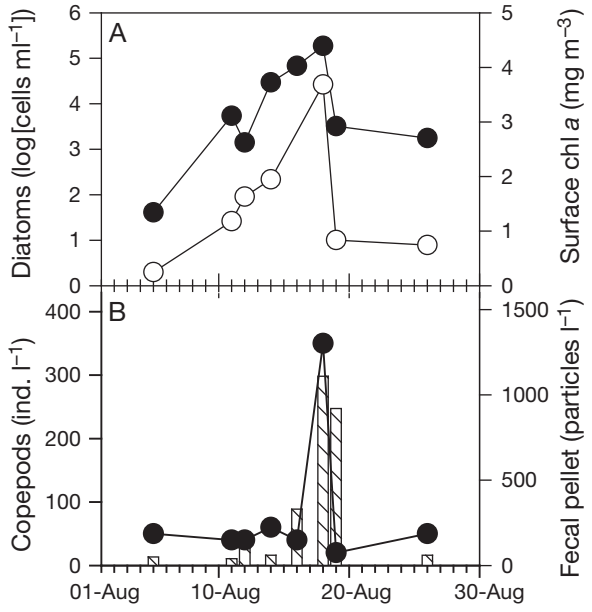

Fig. 6. (A) Surface total diatom abundance (●) and chlorophyll *a* (chl *a*) concentration (○). (B) Surface copepod abundances (●) and their fecal pellet concentrations (bars) at a depth of 50 m

served in the surface layer. Additionally, the fecal pellet counts of copepods were high, with a concentration of approximately 1000 particles l^{-1} in the water sample collected from a depth of 50 m (Fig. 6B). After 24 h, the total diatom abundance dramatically declined 100-fold to 1.8×10^3 cells l^{-1}, which paralleled the decrease in surface chl *a* concentrations (Figs. 4C & 6A).

Relationship between diatom abundances and nutrient concentrations

Without episodic disturbances, the surface water in our study area was oligotrophic, with an N:P ratio >16 (Fig. 7). The diatom abundances pre- and post-Morakot had a significant positive linear relationship with the DIP concentration ($r = 0.77$, $p < 0.01$), but they were not correlated with the DIN concentration ($r = 0.08$, $p = 0.85$; Fig. 7A,B). Moreover, a negative regression between the diatom abundance and the N:P ratios ($r = -0.85$, $p < 0.01$) revealed that water masses with unbalanced low N:P ratios were abundant in diatom cells (Fig. 7C). The surface SiO_4 concentration stayed at high values both pre- and post-Morakot, suggesting that there was sufficient Si for diatom growth, although extra Si was continuously provided by the upwelling and the subsequent riverine flux (Table 1).

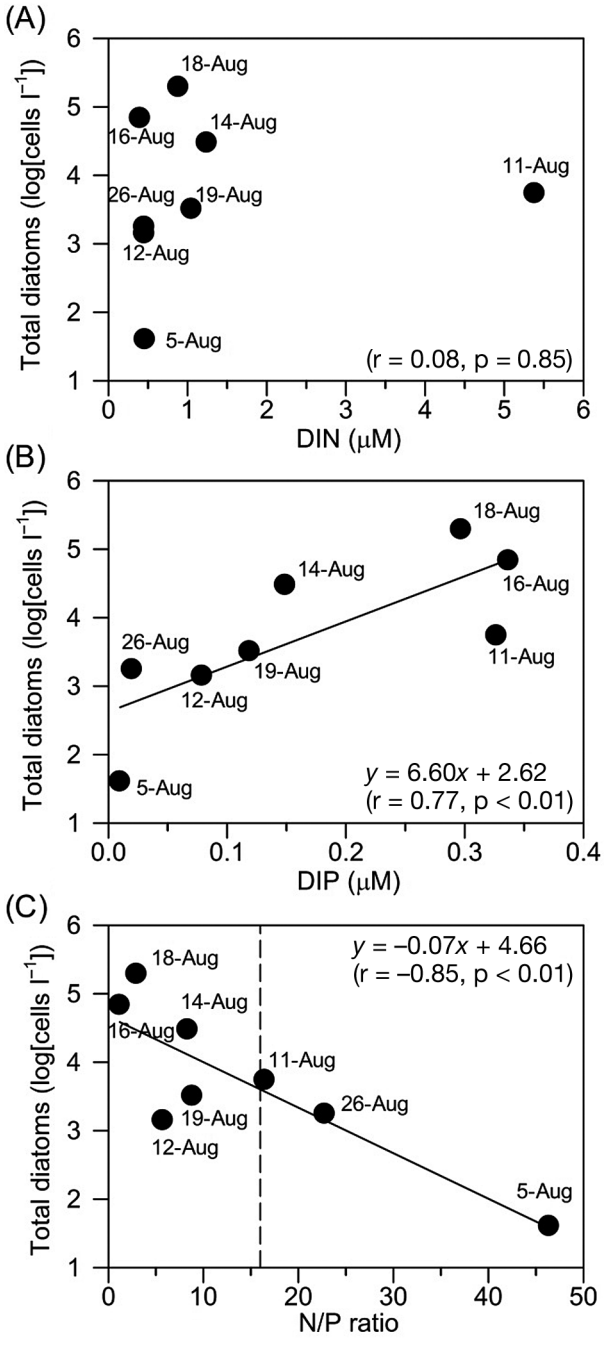

Fig. 7. Linear regression relationships of (A) dissolved inorganic nitrogen (DIN: NO_2+NO_3) concentration, (B) dissolved inorganic phosphorus (DIP) concentration, and (C) molar ratio of DIN and DIP (N:P ratio) versus the diatom abundance in the surface water. All data points were obtained during the cruises conducted in August 2009 (n = 7). The dashed line indicates an N:P ratio of 16

DISCUSSION

Previous studies have indicated that the maximum diatom abundance and chl *a* concentration in the sur-

face water at our study site are 5×10^4 cells l^{-1} and 1 mg m^{-3}, respectively (Chiang et al. 1997, Chen 2000, Gong et al. 2000). Additionally, Hung et al. (2010) reported an upwelling event caused by Typhoon Fengwong that led to an increase in the chl *a* concentration to a peak of 1.4 mg m^{-3} in the same area. However, the influence of Morakot caused an extremely high chl *a* concentration and diatom biomass, 3.7 mg m^{-3} and 1.7×10^5 cells l^{-1}, respectively, compared with previous measurements (Figs. 4 & 6). Strong winds and heavy precipitation usually affect biogeochemical cycles and phytoplankton ecology in the upper waters along the paths of typhoons (Chang et al. 1996, Shiah et al. 2000, Zheng & Tang 2007, Zhao et al. 2008, Chen et al. 2009, Hung et al. 2010). Although several studies have attempted to distinguish the relative importance of these 2 effects on dissolved nutrient enrichment and phytoplankton population dynamics, relevant information is still scarce (Shiah et al. 2000, Paerl et al. 2006, Chen et al. 2009). In contrast to past typhoon events, the disturbances that accompanied Morakot occurred in separate regions, not directly along its path. During the period that Morakot swept over northern Taiwan, strong winds induced an evident upwelling on the shelf break of the southern East China Sea. The rich moisture supply from the large-scale southwestern circulation and the local topographic lifting effects resulted in the record-breaking rainfall in southern Taiwan (Hong et al. 2010). These 2 circumstances led to the uninterrupted supply of dissolved nutrients to our study site and allowed diatoms to thrive.

Deep nutrient-rich water with a balanced N:P ratio of approximately 14 to 17 was brought to the surface derived from the subsurface Kuroshio upwelling and has been suggested to be one of the nutrient sources for microphytoplankton in the southern East China Sea (Gong et al. 1996, Chen 2000, Liu et al. 2010). Although upwelling events occur intermittently off northern Taiwan, the summer monsoon typically drives the formation of a layer of lower-salinity water from the TCWW to suppress the upwelling (Gong et al. 1992, 1996, Wu et al. 2008). Upwelling should not have been prevalent before Morakot because of the frequent summer monsoons (Central Weather Bureau, Taiwan, www.cwb.gov.tw). Without nutrient-rich water derived from the Kuroshio upwelling, the water column was stratified and contained the thriving diazotrophs *Trichodesmium* spp., which led to an elevated N:P ratio (above 40) that was observed before Morakot (Table 2, Fig. 7C). When typhoons draw near to northeastern Taiwan, the counterclockwise winds push the Kuroshio waters toward the shelf break and subsequently induce an evident upwelling event in this region (Chen et al. 2003). This phenomenon was observed after Morakot, and a similar scenario has also been described by Chang et al. (2008) and Hung et al. (2010) in the same area. The upwelling water balanced the surface N:P ratio near the Redfield stoichiometric value of 16 and created an appropriate environment for diatom prosperity (Hecky & Kilham 1988, Arrigo 2005).

After the upwelling event, plentiful floodwater with the TCWW reached our study site and reduced the salinity to below 33, which had never been observed in this region previously (Chen 2000, Gong et al. 2000). Besides the terrestrial dissolved inorganic nutrients carried with the run-off, a total of 3.8 to 8.4 Tg of coarse woody debris, which contained massive amounts of organic material, was simultaneously transported northward from the flooding regions (West et al. 2011). In summer, the TCWW, with a low N:P ratio (between 5.4 and 7.6), has been suggested to be an important phosphate source in the southern East China Sea (Liu et al. 2000, Chung et al. 2001, Naik & Chen 2008). This phenomenon should be strengthened due to the strong southwest wind that occurred while Morakot passed through the Taiwan Strait. Although the T–S diagrams showed that the less-saline water mass over the upper layer was present on 18 and 19 August, the elevated surface DIP suggested that the arrival of riverine flux occurred on 14 August, which is nearly consistent with the deduction estimated from the velocity of the TCWW at 40 cm s^{-1} (Chung et al. 2001). The nutrient concentrations in the upper water column quickly returned to low levels when the upwelling event ceased. Nevertheless, the delayed riverine flux consecutively provided ample nutrients, DIP in particular, for large centric diatom growth and sustained the bloom development following the upwelling event.

Turbid floodwaters can reduce light transmission in the water column and result in the disruption of phytoplankton growth in estuaries and coasts (Cole & Cloern 1984, Lane et al. 2002, Paerl et al. 2006). Although the relative bio-optical information was deficient on 14 August while the riverine flux emerged, the available data of surface particle transmission showed a significant negative relationship with the concentrations of chl *a* ($r = -0.96$, $p < 0.01$). This relationship suggested that the decrease in light transmission ability could be attributed to the rise in phytoplankton biomass. This implication was also supported by the appearance of the shallowest euphotic zone with a high integrated chl *a* concentration on 18 August (Table 1).

High NO_2 concentrations were also detected in the surface waters when the low-salinity waters intruded after Morakot (Table 1). In addition to a direct supply from land and excretion by phytoplankton, nitrification by chemoautotrophic bacteria provides another mechanism for the accumulation of NO_2 in the surface layer (Zehr & Ward 2002, Lomas & Lipschultz 2006, Naik & Chen 2008). Because energy is required to reduce NO_3 to NH_4 through nitrogen assimilation, phytoplankton generally prefer to take up reduced nitrogen compounds, rather than NO_3, as their nitrogen source. Tada et al. (2009) found that the diatom *Skeletonema costatum* had a faster growth rate using NH_4 than NO_3 in Dokai Bay, Japan. The complete inhibition of NO_3 transporter gene expression by the addition of NH_4 supports this hypothesis (Kang et al. 2009). Therefore, the reduced nitrogen compounds in the invading water mass should also contribute to the diatom bloom.

Because the doubling time of phytoplankton is typically within hours, the observed population dynamics are most likely attributable to *in situ* growth (McKinnon et al. 2003). Without episodic disturbances, diatoms are not the most abundant microphytoplankton in the study area during the summer. With nutrient inputs from upwelling, the microphytoplankton assemblages primarily consist of *Chaetoceros* spp. and *Nitzschia* spp. (Chiang et al. 1997), and a similar phenomenon was also observed after the upwelling event caused by Morakot. When the low-salinity waters intruded, *Chaetoceros* spp. still showed an exponential growth trend with a growth rate of 0.67 d^{-1}, in contrast to pennate diatoms, which remained at a steady growth rate (Table 2). Although Chen et al. (2009) reported an opposite trend in diatom succession in the oligotrophic Kuroshio waters after the passages of 3 typhoons, the total combined cell density of pennate and centric diatoms was only 3.8×10^2 cells l^{-1}, which is approximately 1000 times lower than the measurement of this study. This result implies that the magnitude of the dissolved nutrient supply not only determines the abundance of microphytoplankton but also influences their assemblages.

Events of massive cell loss often occur following phytoplankton blooms. Herbivore grazing, sedimentation, and self-destructive lysis are considered the main causes for the decline of phytoplankton blooms (Brussaard et al. 1995, Kiørboe et al. 1998, Chung et al. 2005, Sarthou et al. 2005). In this study, the diatom bloom terminated within 24 h. After the bloom, the sinking particles collected below the euphotic zone (50 m) by floating traps consisted primarily of fecal pellets. Cell debris and aggregative particles were not observed in this sample (C.C. Hung unpubl. data). This result corresponded to our observation and suggested that the termination of the diatom bloom was caused by intense grazing pressure by copepods, rather than nutrient depletion or self-destructive lysis. Previous studies have also implicated zooplankton grazing as an important factor for regulating the diatom abundance in this area (Chen & Chen 1992, Chiang et al. 1997). The generation time of zooplankton is typically more than 1 wk. Therefore, the emergence of copepods should be due to advection into our study site (McKinnon et al. 2003). This biological process during and after the diatom bloom not only led to a more dominant grazing food chain but also facilitated the sinking flux of POC. Moreover, the northward TCWW is the major current off northern Taiwan in the summer (Jan et al. 2010, 2011). In addition to grazing effects, the possibility of dilution with peripheral water masses should also be considered an influencing factor in diminishing the phytoplankton biomass in a short period of time.

The advantage of serial *in situ* measurements before and after typhoons is the ability to acquire information on the succession of hydrographic properties and phytoplankton population dynamics. In this study, we clearly described how the upwelling and consecutive terrestrial inputs caused by Typhoon Morakot jointly enhanced the dissolved nutrient concentrations and stimulated a diatom bloom. By consuming diatoms, copepods accelerated the sinking flux of POC and promoted the grazing food chain. Our data compensate for the limitation of satellite remote sensing observations and provide a more comprehensive understanding of biogeochemical responses to the episodic disturbances induced by typhoons.

Acknowledgements. We thank J. Chang, W.C. Chou and S. Jan for their comments and suggestions. The positive comments of the responsible editor and the 4 anonymous reviewers are deeply appreciated. We also thank the captains and crew of RV 'Ocean Researcher II' and the fishing boat 'Yang-Ming' for their assistance. This work was supported by the National Science Council of Taiwan, NSC99-2611-M-019-014-MY2, and the Center of Excellence for Marine Bioenvironment and Biotechnology of the National Taiwan Ocean University.

LITERATURE CITED

Arrigo KR (2005) Marine microorganisms and global nutrient cycles. Nature 437:349–355

Babin SM, Carton JA, Dickey TD, Wiggert JD (2004) Satellite evidence of hurricane-induced phytoplankton blooms in an oceanic desert. J Geophys Res 109:C03043

Brussaard CPD, Riegman R, Noordeloos AAM, Cadée GC and others (1995) Effects of grazing, sedimentation and phytoplankton cell lysis on the structure of a coastal pelagic food web. Mar Ecol Prog Ser 123:259–271

Byju P, Kumar SP (2011) Physical and biological response of the Arabian Sea to tropical cyclone Phyan and its implications. Mar Environ Res 71:325–330

Chang J, Chung CC, Gong GC (1996) Influences of cyclones on chlorophyll *a* concentration and *Synechococcus* abundance in a subtropical western Pacific coastal ecosystem. Mar Ecol Prog Ser 140:199–205

Chang J, Chiang KP, Gong GC (2000) Seasonal variation and cross-shelf distribution of the nitrogen-fixing cyanobacterium, *Trichodesmium*, in southern East China Sea. Cont Shelf Res 20:479–492

Chang Y, Liao HT, Lee MA, Chan JW and others (2008) Multisatellite observation on upwelling after the passage of typhoon Hai-Tang in the southern East China Sea. Geophys Res Lett 35:L03612

Chen CTA, Liu CT, Chuang WS, Yang YJ, Shiah FK, Tang TY, Chung SW (2003) Enhanced buoyancy and hence upwelling of subsurface Kuroshio waters after a typhoon in the southern East China Sea. J Mar Syst 42:65–79

Chen HY, Chen YLL (1992) Quantity and quality of summer surface net zooplankton in the Kuroshio current-induced upwelling northeast of Taiwan. Terr Atmos Ocean Sci 3:321–334

Chen YLL (2000) Comparisons of primary productivity and phytoplankton size structure in the marginal regions of southern East China Sea. Cont Shelf Res 20:437–458

Chen YLL, Chen HY, Jan S, Tuo SH (2009) Phytoplankton productivity enhancement and assemblage change in the upstream Kuroshio after typhoons. Mar Ecol Prog Ser 385:111–126

Chiang KP, Shiah FK, Gong GC (1997) Distribution of summer diatom assemblages in and around a local upwelling in the East China Sea northeast of Taiwan. Bot Bull Acad Sin 38:121–129

Chung CC, Hwang SPL, Chang J (2005) Cooccurrence of *ScDSP* gene expression, cell death, and DNA fragmentation in a marine diatom, *Skeletonema costatum.* Appl Environ Microbiol 71:8744–8751

Chung CC, Chang J, Gong GC, Hsu SC, Chiang KP, Liao CW (2011) Effects of Asian dust storms on *Synechococcus* populations in the subtropical Kuroshio Current. Mar Biotechnol 13:751–763

Chung SW, Jan S, Liu KK (2001) Nutrient fluxes through the Taiwan Strait in spring and summer 1999. J Oceanogr 57:47–53

Cole BE, Cloern JE (1984) Significance of biomass and light availability to phytoplankton productivity in San Francisco Bay. Mar Ecol Prog Ser 17:15–24

Elsner JB, Kossin JP, Jagger TH (2008) The increasing intensity of the strongest tropical cyclones. Nature 455:92–95

Falkowski PG, Oliver MJ (2007) Mix and match: how climate selects phytoplankton. Nat Rev Microbiol 5: 813–819

Gong GC, Shyu CZ, Shih WH, Liu KK (1992) Temperature fluctuation on the cold water off northern Taiwan: June–December, 1990. Acta Oceanogr Taiwan 28:118–127

Gong GC, Lee Chen YL, Liu KK (1996) Chemical hydrography and chlorophyll a distribution in the East China Sea in summer: implications in nutrient dynamics. Cont Shelf Res 16:1561–1590

Gong GC, Chang J, Wen YH (1999) Estimation of annual primary production in the Kuroshio waters northeast of Taiwan using a photosynthesis-irradiance model. Deep-Sea Res I 46:93–108

Gong GC, Shiah FK, Liu KK, Wen YH, Liang MH (2000) Spatial and temporal variation of chlorophyll *a*, primary productivity and chemical hydrography in the southern East China Sea. Cont Shelf Res 20:411–436

Gong GC, Wen YH, Wang BW, Liu GJ (2003) Seasonal variation of chlorophyll *a* concentration, primary production and environmental conditions in the subtropical East China Sea. Deep-Sea Res II 50:1219–1236

Gong GC, Liu KK, Chiang KP, Hsiung TM and others (2011) Yangtze River floods enhance coastal ocean phytoplankton biomass and potential fish production. Geophys Res Lett 38:L13603

Hecky RE, Kilham P (1988) Nutrient limitation of phytoplankton in freshwater and marine environments: a review of recent evidence on the effects of enrichment. Limnol Oceanogr 33:796–822

Hoegh-Guldberg O, Bruno JF (2010) The impact of climate change on the world's marine ecosystems. Science 328: 1523–1528

Hoge F, Lyon PE (2002) Satellite observation of chromophoric dissolved organic matter (CDOM) variability in the wake of hurricanes and typhoons. Geophys Res Lett 29:141–144

Hong CC, Lee MY, Hsu HH, Kuo JL (2010) Role of submonthly disturbance and 40–50 day ISO on the extreme rainfall event associated with Typhoon Morakot (2009) in Southern Taiwan. Geophys Res Lett 37:L08805

Hung CC, Gong GC (2011) Biogeochemical responses in the southern East China Sea after typhoons. Oceanography 24:42–51

Hung CC, Gong GC, Chung WC, Kuo WT, Lin FC (2009) Enhancement of particulate organic carbon export flux induced by atmospheric forcing in the subtropical oligotrophic northwest Pacific Ocean. Mar Chem 113:19–24

Hung CC, Gong GC, Chou WC, Chung CC and others (2010) The effect of typhoon on particulate organic carbon flux in the southern East China Sea. Biogeosciences 7:3007–3018

Jan S, Tseng YH, Dietrich D (2010) Sources of water in the Taiwan Strait. J Oceanogr 66:211–221

Jan S, Chen CC, Tsai YL, Yang YJ and others (2011) Mean structure and variability of the cold dome northeast of Taiwan. Oceanography 24:100–109

Jickells TD, An ZS, Andersen KK, Baker AR and others (2005) Global iron connections between desert dust, ocean biogeochemistry, and climate. Science 308:67–71

Kang LK, Hwang SPL, Lin HJ, Chen PC, Chang J (2009) Establishment of minimal and maximal transcript levels for nitrate transporter genes for detecting nitrogen deficiency in the marine phytoplankton *Isochrysis galbana* (Prymnesiophyceae) and *Thalassiosira pseudonana* (Bacillariophyceae). J Phycol 45:864–872

Karl DM, Bidigare RR, Letelier RM (2001) Long-term changes in plankton community structure and productivity in the North Pacific Subtropical Gyre: the domain shift hypothesis. Deep-Sea Res II 48:1449–1470

Kiørboe T, Tiselius P, Mitchell-Innes B, Hansen J, Visser A, Mari X (1998) Intensive aggregate formation with low vertical flux during an upwelling-induced diatom bloom. Limnol Oceanogr 43:104–116

Lane R, Day J, Marx B, Reves E, Kemp G (2002) Seasonal and spatial water quality changes in the outflow plume

of the Atchafalaya River, Louisiana, USA. Estuaries 25: 30–42

Levitus S (1982) Climatological atlas of the world ocean. NOAA professional paper. National Oceanic and Atmospheric Administration, Seattle, WA

Liu HC, Gong GC, Chang J (2010) Lateral water exchange between shelf-margin upwelling and Kuroshio waters influences phosphorus stress in microphytoplankton. Mar Ecol Prog Ser 409:121–130

Liu KK, Tang TY, Gong GC, Chen LY, Shiah FK (2000) Cross-shelf and along-shelf nutrient fluxes derived from flow fields and chemical hydrography observed in the southern East China Sea off northern Taiwan. Cont Shelf Res 20:493–523

Lomas MW, Lipschultz F (2006) Forming the primary nitrite maximum: nitrifiers or phytoplankton? Limnol Oceanogr 51:2453–2467

Lorenzen CJ (1972) Extinction of light in the ocean by phytoplankton. ICES J Mar Sci 34:262–267

McKinnon AD, Meekan MG, Carleton JH, Furnas MJ, Duggan S, Skirving W (2003) Rapid changes in shelf waters and pelagic communities on the southern Northwest Shelf, Australia, following a tropical cyclone. Cont Shelf Res 23:93–111

Naik H, Chen CTA (2008) Biogeochemical cycling in the Taiwan Strait. Estuar Coast Shelf Sci 78:603–612

Paerl HW, Valdes LM, Peierls BL, Adolf JE, Harding LWJ (2006) Anthropogenic and climatic influences on the eutrophication of large estuarine ecosystems. Limnol Oceanogr 51:448–462

Parsons TR, Maita Y, Lalli CM (1984) A manual of chemical and biological methods for seawater analysis. Pergamon Press, New York, NY

Pielou EC (1966) Species-diversity and pattern-diversity in the study of ecological succession. J Theor Biol 10: 370–383

Sarthou G, Timmermans KR, Blain S, Treguer P (2005) Growth physiology and fate of diatoms in the ocean: a review. J Sea Res 53:25–42

Shang SL, Li FS, Wu J, Hu C and others (2008) Changes of temperature and bio-optical properties in the South China Sea in response to typhoon Lingling, 2001. Geophys Res Lett 35:L10602

Shannon CE (1948) A mathematical theory of communication. Bell Syst Tech J 27:379–423

Shi W, Wang M (2007) Observations of a hurricane Katrina-induced phytoplankton bloom in the Gulf of Mexico. Geophys Res Lett 34:L11607

Shiah FK, Chung SW, Kao SJ, Gong GC, Liu KK (2000) Biological and hydrographical responses to tropical cyclones (typhoons) in the continental shelf of the Taiwan Strait. Cont Shelf Res 20:2029–2044

Siswanto E, Morimoto A, Kojima S (2009) Enhancement of phytoplankton primary productivity in the southern East China Sea following episodic typhoon passage. Geophys Res Lett 36:L11603

Tada K, Suksomjit M, Ichimi K, Funaki Y, Montani S, Yamada M, Harrison P (2009) Diatoms grow faster using ammonium in rapidly flushed eutrophic Dokai Bay, Japan. J Oceanogr 65:885–891

Tang S, Chen C, Zhan H, Zhang J, Yang J (2008) An appraisal of surface chlorophyll estimation by satellite remote sensing in the South China Sea. Int J Remote Sens 29:6217–6226

Tomas C, Hasle G, Syvertsen E, Steidinger K, Tangen K (1996) Identifying marine diatoms and dinoflagellates. Academic Press, San Diego, CA

Vinayachandran PN, Mathew S (2003) Phytoplankton bloom in the Bay of Bengal during the northeast monsoon and its intensification by cyclones. Geophys Res Lett 30:1572

Walker ND, Leben RR, Balasubramanian S (2005) Hurricane-forced upwelling and chlorophyll *a* enhancement within cold-core cyclones in the Gulf of Mexico. Geophys Res Lett 32:L18610

West AJ, Lin CW, Lin CT, Hilton RG and others (2011) Mobilization and transport of coarse woody debris to the oceans triggered by an extreme tropical storm. Limnol Oceanogr 56:77–85

Wu CR, Lu HF, Chao SY (2008) A numerical study on the formation of upwelling off northeast Taiwan. J Geophys Res 113:C08025

Yuan J, Miller RL, Powell RT, Dagg MJ (2004) Storm-induced injection of the Mississippi River plume into the open Gulf of Mexico. Geophys Res Lett 31:L09312

Zehr JP, Ward BB (2002) Nitrogen cycling in the ocean: new perspectives on processes and paradigms. Appl Environ Microbiol 68:1015–1024

Zhao H, Tang D, Wang Y (2008) Comparison of phytoplankton blooms triggered by two typhoons with different intensities and translation speeds in the South China Sea. Mar Ecol Prog Ser 365:57–65

Zheng GM, Tang D (2007) Offshore and nearshore chlorophyll increases induced by typhoon winds and subsequent terrestrial rainwater runoff. Mar Ecol Prog Ser 333: 61–67

Editorial responsibility: Graham Savidge, Portaferry, UK

Submitted: May 2, 2011; Accepted: November 9, 2011
Proofs received from author(s): February 10, 2012